

## The nature of red luminescence of natural benitoite $\text{BaTiSi}_3\text{O}_9$

M. Gaft<sup>1</sup>, L. Nagli<sup>2</sup>, G. Waychunas<sup>3</sup>, and G. Panczer<sup>4</sup>

<sup>1</sup> Laser Detection Systems (LDS), Rishon-Lezion, and  
The Open University of Israel, Raanana, Israel

<sup>2</sup> School of Physics and Astronomy, Tel-Aviv University, Tel-Aviv, Israel

<sup>3</sup> Geochemistry Department, Aqueous Geochemistry Group,  
Earth Sciences Division MS 70-108B E.O. Lawrence Berkeley  
National Laboratory, Berkeley, CA, USA

<sup>4</sup> Physical Chemistry of Luminescence Materials Laboratory,  
Lyon 1 University, UMR 5620 CNRS, Villeurbanne, France

Received January 7, 2005; revised version accepted May 27, 2005  
Editorial handling: E. Libowitzky and A. Beran

### Summary

This work examines the red luminescence of benitoite studied by laser-induced time-resolved luminescence spectroscopy. This method allows the differentiation between luminescence centers of similar emission wavelengths, but different decay times. We have also examined the luminescence intensity and decay time as a function of temperature. We found that the red emission of benitoite consists of two individual bands and one line and suggest that the activators of luminescence in benitoite system are  $\text{Ti}^{3+}$  and a  $d^3$  element, namely  $\text{Cr}^{3+}$  or  $\text{Mn}^{4+}$ .

### Introduction

Benitoite,  $\text{BaTiSi}_3\text{O}_9$ , is a cyclosilicate mineral belonging to space group  $D_{3h}^2$ - $P6c2$  with two formula units per unit cell. Its ditrigonal bipyramidal structure is based upon three  $\text{SiO}_4$  tetrahedra, each sharing two of their oxygen atoms to form rings. The Ba and Ti atoms lie on trigonal axes parallel to the c-axis in two-fold positions on either side of a mirror plane, respectively. Titanium is octahedrally coordinated to the oxygen atoms, while each oxygen atom of the  $\text{TiO}_6$  octahedron comes from an unshared corner of a trimeric  $[\text{Si}_3\text{O}_9]^{6-}$  ring. Barium also has six-fold coordination. The mean distance Ti–O is 1.94 Å, and for Ba–O it is 2.77 Å. Six other oxygen atoms are located about 3.43 Å from the Ba site, but

evidently they cannot be considered as belonging to the first coordination sphere of Ba.

The measured amounts of Ba, Ti, and Si in benitoite are remarkably constant ( $\text{BaO} = 37.09\%$ ,  $\text{SiO}_2 = 43.59\%$ ,  $\text{TiO}_2 = 19.32\%$ ), regardless of color or locality, and are near the ideal values that are calculated from the chemical formula. The greatest chemical variation in benitoite was detected for tin, up to 4.1% tin oxide can be incorporated. A zirconium-bearing blue benitoite was found to contain 1.77 wt.%  $\text{ZrO}_2$ . Other elements show minor variations, most notably Nb, Na, Ca, K, V, Sr, Al and Fe (*Lauris et al.*, 1997; *Laird and Albee*, 1972).

Numerous investigations have attempted to link the chemical composition of benitoite to its coloration. Detailed microprobe and emission spectroscopy analysis indicated that the concentrations of major and minor elements of the white and blue parts of the crystal were very similar. In an attempt to account for the color of the mineral a careful examination of a two-gram portion of the blue mineral failed to show the presence of appreciable amounts of iron, cobalt, manganese, copper or chromium (*Louderback*, 1909). In spite of many studies on the chemical composition of benitoite, no correlation has been found between intensity of color and any minor or trace element.

Useful information for luminescence interpretation may however, be obtained from optical absorption spectroscopy, which reveals the excited energy levels. Optical spectroscopy of blue benitoite reveals a broad absorption band peaking at  $\sim 700$  nm, most of which is in the near-infrared region (*Rossmann*, 1997). In spite of much effort to interpret the spectral data, the cause of blue color in benitoite remains elusive. Attempts to bleach the color by heat treatment were unsuccessful; thus its origin has been considered as rather due to a paramagnetic impurity than to an electron trapped at an anion vacancy. Possible explanations are  $\text{Fe}^{2+}-\text{Ti}^{4+}$  or  $\text{Fe}^{2+}-\text{Fe}^{3+}$  inter-valance charge transfer processes (*Rossmann*, 1997), especially because traces of  $\text{Fe}^{3+}$  have been found in benitoite by EPR (*Vassilikou-Dova and Eftaxias*, 1991).

Benitoite is a well-known luminescent mineral. Its cathodoluminescence is always intense blue. The ultraviolet response of benitoite is diverse. Under short-wave excitation of a mercury lamp at 254 nm, benitoite fluorescence is intense blue-white. The fluorescence of the paler-colored cores is frequently more vivid than the edges. This blue emission is associated with intrinsic  $\text{TiO}_6$  centers (*Gaft et al.*, 2004). Under long-wave UV excitation at 365 nm, red luminescence sometimes appears, and is more pronounced in colorless and lighter-colored benitoite specimens. The spectral-kinetic properties of this red emission have not been studied and its nature has not been interpreted. Hence in the present work we have conducted a detailed investigation of the benitoite red luminescence in order to understand its origin. Most of the experimental studies and analyses of spectral-kinetic properties of red emission bands have been done in the temperature range of 30–450 K. Laser-induced time-resolved spectroscopy was the principal tool, which allows discrimination between centers with emission in the same spectral range, but with different decay times. This method involves recording the intensity in a specific time gate at a given delay after the excitation pulse. Such manipulation allows to avoid overlapping of emission bands produced from different centers.

## Experimental

The time-resolved luminescence spectra were investigated under excimer HeCl (308 nm), nitrogen (337 nm) and 2<sup>nd</sup>, 3<sup>rd</sup> and 4<sup>th</sup> Nd-YAG harmonics (532, 355 and 266 nm, correspondingly) pulsed lasers excitations, which deliver pulses of 8–10 ns duration and 0.1 cm<sup>-1</sup> spectral width. The spectra observed at 90° geometry were analyzed by iStar equipment enabling time-resolved spectra acquisition with the following features: delay times and strobe pulse duration 1 ns – 19 ms, spectral detection range 200–900 nm (1200 channels, spectral resolution 0.5–1 nm, gratings with 300 and 600 lines/mm), detector type – intensified CCD matrix.

The steady-state luminescence spectra were studied under nitrogen laser (337 nm) and UV He lamp excitations. In the luminescence decay investigation, the forth harmonic (266 nm) of a Nd-YAG pulsed laser was used as the excitation source, while the sample luminescence was analyzed by a grating monochromator. A digital oscilloscope processed the output from the photomultiplier.

Luminescence spectra and decay times were measured at temperatures from 30 to 300 K.

For optical measurements natural polished and unpolished benitoite samples were used. The optical absorption spectra in the spectral range from 190 to 1100 nm were recorded using a Jasco spectrophotometer (model V-530). All absorption spectra are unpolarized and recorded at 300 K.

Five benitoite samples have been studied; one white, one opaque blue, one transparent of gem quality with blue color, and two colorless almost transparent specimens. All five have been checked by Raman and breakdown spectroscopy to ensure that we are dealing with benitoite. This was done with the same experimental equipment used for luminescence adding a notch filter and focusing lens.

## Results and discussion

### *Complexity of the red emission*

The strongest red luminescence has been found mainly in transparent samples. Figure 1 represents the absorption spectrum of the transparent sample in which all detected red emissions are most intense. It does not contain the broadband absorption peaking at 750 nm, which is responsible for the blue benitoite color (Rossman, 1997). We have detected intense UV bands in all samples studied, which are evidently due to electronic transitions in TiO<sub>6</sub> centers and accompanied by strong blue emission (Gaft et al., 2004). The broad intense band in the NIR part of the spectrum may influence benitoite color and is similar to bands observed in blue rutile that may be the result of small polaron Ti<sup>3+</sup>Ti<sup>4+</sup> charge transfer (Khomenko et al., 1998).

Figure 2a represents the steady state luminescence spectrum of the same benitoite sample as in Fig. 1 under excitation at 337 nm. At room temperature it contains a very broad, relatively weak asymmetric band. At lower temperatures the band is much narrower and more symmetric, the intensity increases and a narrow line at 682 nm appears. The same sample under excitation at 355 nm at

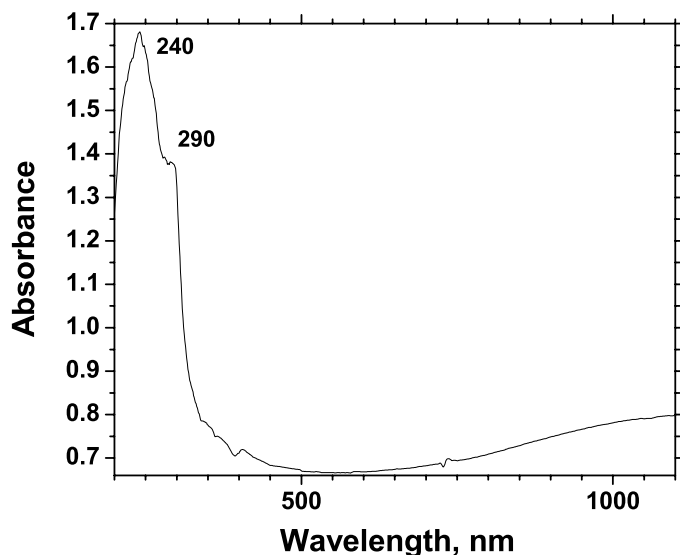


Fig. 1. Absorption spectrum of transparent benitoite with most intensive red emissions

300 K is characterized by stronger emission with a broad asymmetric band accompanied by the line at 682 nm (Fig. 2b). Another transparent sample with slightly bluish color under excitation at 355 nm at 300 K exhibits a much narrower red band (Fig. 2c). These observations suggest the presence of two different broad bands, peaking at approximately 650 and 730 nm respectively, and a narrow line at 682 nm with different relative intensities in different samples. At lower temperatures the band at 650 nm and the narrow line become much stronger, while the band at 730 nm is considerably weaker. Time-resolved luminescence spectroscopy confirmed the presence of several separate luminescence centers with different spectra and decays, and enables to separate and study them in pure form. Each luminescence center will be considered separately.

#### *Emission band at 650 nm – $Ti^{3+}$ related luminescence*

This band was found in one of the transparent samples where it is excited not only by UV laser, but also by conventional UV lamp. In this sample and in a bluish transparent one it dominates the spectrum and may be detected even by steady-state spectroscopy. In other samples it may be selected only by time-resolved spectroscopy using a narrow gate. At room temperature this band has a maximum at 650 nm with a half-width of  $\sim 135$  nm and may be approximated by one Gaussian function (Fig. 3a). One exponent with a decay time of  $1.1 \mu s$  approximates well its decay curve at room temperature (Fig. 3b). At lower temperatures up to 40 K the red luminescence intensity is approximately 10 times higher, and the spectrum undergoes certain changes, namely its maximum shifts to 668 nm and the band becomes a little narrower with a half-width of  $\sim 105$  nm (Fig. 3c). Such red emission is not excited by laser sources in the visible part of the spectrum, such as 488, 514 and 532 nm. The excitation spectrum at lower temperatures, when

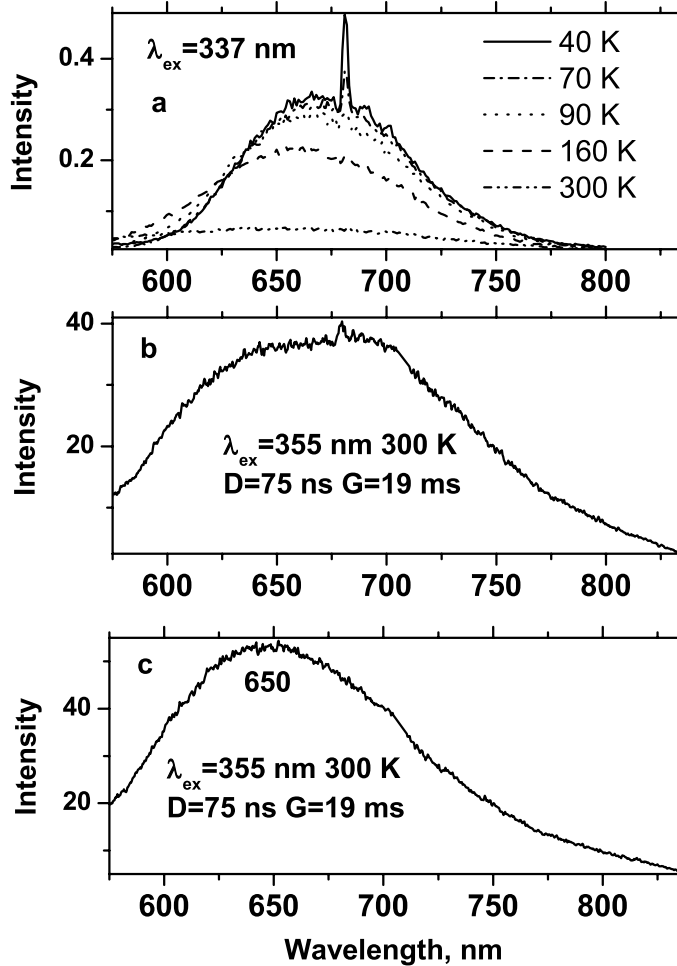


Fig. 2. Typical steady-state red luminescence spectra of benitoite: **a** transparent benitoite under 337 nm excitation at different temperatures; **b** the same sample as for **a** under 355 nm excitation at 300 K; **c** bluish transparent sample under 355 nm excitation at 300 K

luminescence intensity is strong enough to use a UV lamp source, contains one asymmetric band peaking at  $\sim 350 \text{ nm}$  with half-width of  $\sim 75 \text{ nm}$  (Fig. 3c), and the corresponding Stokes shift is approximately  $13000 \text{ cm}^{-1}$ . The spectrum can be approximated by two Gaussian curves peaking at  $28130 \text{ cm}^{-1}$  (355 nm) and  $30279 \text{ cm}^{-1}$  (330 nm) respectively. The decay curve at lower temperatures remains mono-exponential, but the decay time becomes substantially longer ( $\sim 20 \mu\text{s}$ ) (Fig. 3d).

Figure 4 summarizes the temperature dependence of the decay time  $\tau$  (squares) and relative quantum yield  $\eta$  (circles) of the red benitoite luminescence at 650 nm in the forms of  $\tau$  and  $\eta$  as functions of  $1/T$ . The relative quantum yield at a specific temperature (T) was calculated as:

$$\eta(T) = I_0(T)/I_0(30 \text{ K}) \quad (1)$$

where  $I_0$  is the maximum luminescence intensity at the corresponding temperature. The luminescence may be explained by using a simple scheme with two levels,

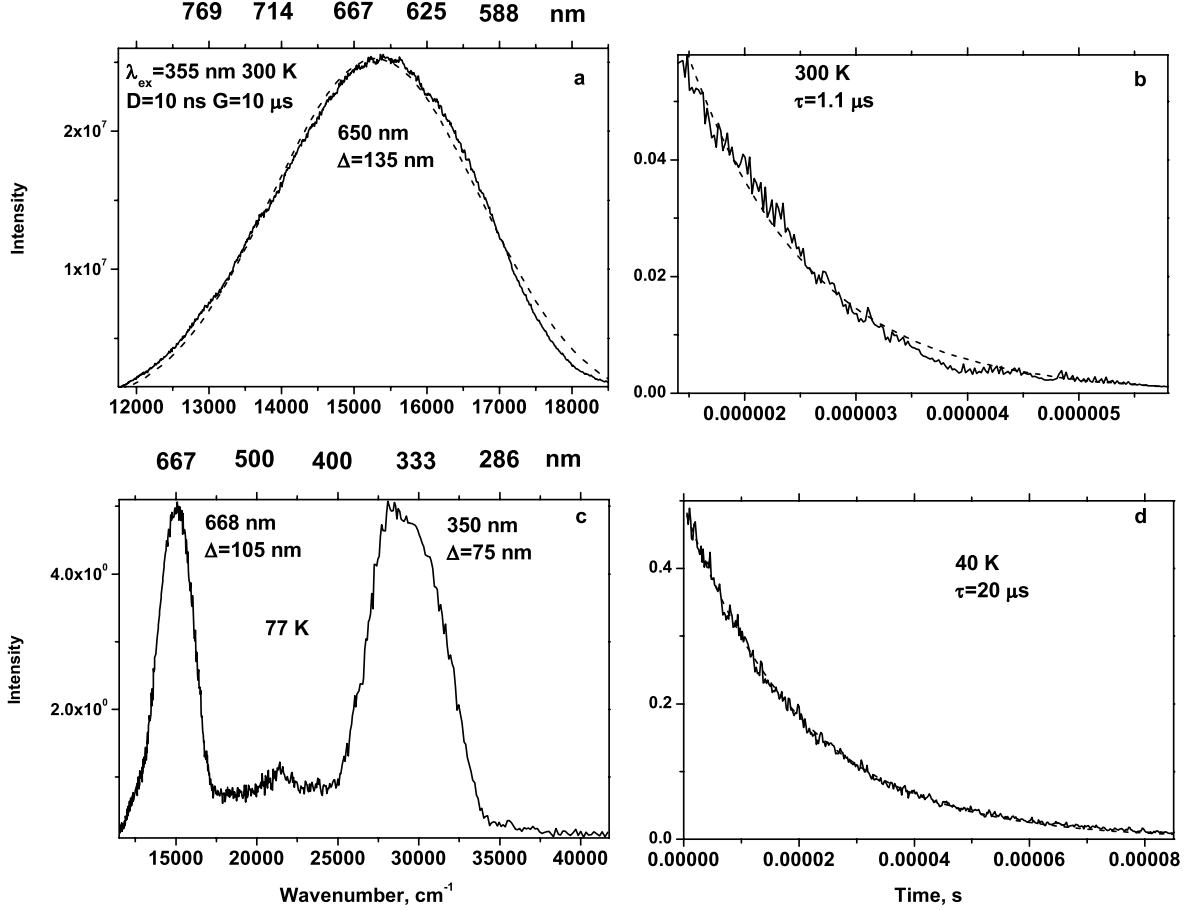


Fig. 3. Red luminescence band peaking at 650 nm: **a** luminescence spectrum at 300 K approximated by one Gaussian curve; **b** decay time curve at 300 K approximated by one exponent with  $\tau = 1.1 \mu\text{s}$ ; **c** luminescence and excitation spectra at 40 K; **d** decay time curve at 40 K approximated by one exponent with  $\tau = 20 \mu\text{s}$

excited and ground states. The relative quantum yield and decay time of the red emission may be described by simple Arrhenius equations:

$$\eta = \frac{1}{1 + A_d/A_r \exp(-U/kT)} \quad (2)$$

$$\tau = \frac{1}{A_r + A_d \exp(-U/kT)} \quad (3)$$

where  $A_r$  and  $A_d$  are radiation and non-radiation transition probabilities between excited and ground states, and  $U$  is the energetic barrier between them. The best fit to the experimental results is obtained when  $A_r = 5.4 \times 10^4 \text{ s}^{-1}$ ,  $A_d = 2.66 \times 10^7 \text{ s}^{-1}$  and  $U = 0.09 \text{ eV}$ . Two competing processes take place after excitation: emission with radiative probability  $A_r$  and non-radiative quenching due to energetic barrier  $U$  with probability  $A_d \exp(-U/kT)$ . At low temperatures the radiative process dominates and the relative quantum yield is relatively higher and decay time is

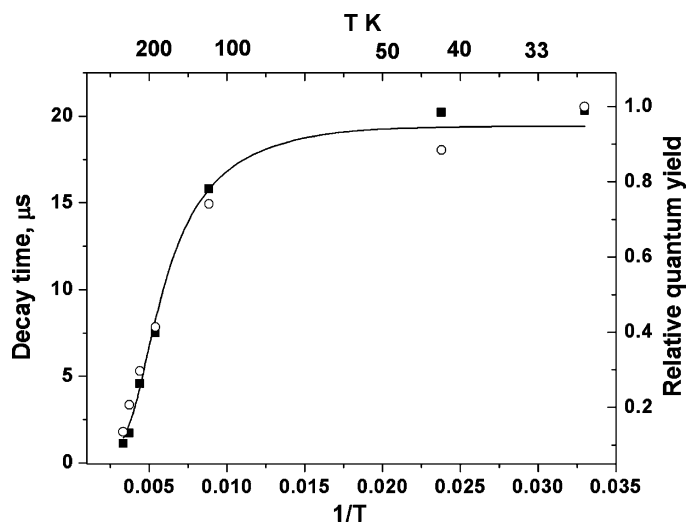


Fig. 4. Temperature dependence of relative quantum yield  $\eta$  circles and decay time  $\tau$  squares of the red emission band of benitoite at 650 nm

relatively long. At elevated temperatures the non-radiative mechanism dominates with increased fluorescence quenching and shortened decay time.

Because this red luminescence band is relatively rare, it must not be associated with the regular components of the benitoite structure. The possible luminescence centers may be impurities or structural defects in the crystal. From previous studies, the following red emission impurity centers may be supposed to be present in benitoite:  $\text{Bi}^{3+}$ ,  $\text{Bi}^{2+}$ ,  $\text{Ag}^+$ ,  $\text{Cu}^+$  substituting for  $\text{Ba}^{2+}$ ;  $\text{Cr}^{3+}$ ,  $\text{Mn}^{4+}$  and  $\text{Ti}^{3+}$  in  $\text{Ti}^{4+}$  position; and  $\text{Fe}^{3+}$  substituting for  $\text{Si}^{4+}$  (Gaft et al., 2001, 2003). The latter one may be excluded, because d–d transitions in  $\text{Fe}^{3+}$  centers are strongly forbidden and have a very long decay time of several ms, while the red benitoite luminescence has a much shorter decay time of several  $\mu\text{s}$ . Making an attempt to correlate the red benitoite luminescence with specific impurities, three benitoite samples have been analyzed by ICP method. Traces of Bi have not been found. The detected impurities with possible broadband red luminescence are Cr, Mn, and Cu (Table 1). Comparison of the luminescence intensity at 650 nm in different samples reveals that any correlation is absent with these impurities. Besides, their energy levels schemes do not correspond to relative quantum yield and decay time behavior, described in Fig. 4.

Thus it is supposed that the most probable luminescence center is  $\text{Ti}^{3+}$ , which has not been confidently identified in other minerals yet, but is well known in tunable laser systems. Its presence is quite natural in Ti-bearing benitoite. The

Table 1. Concentrations of some trace elements (ppm) in benitoite

Sample	$^{55}\text{Mn}$	$^{65}\text{Cu}$	$^{53}\text{Cr}$	$^{52}\text{Cr}$
Blue	1.58	1109.18	49.3	51.51
Bluish	10.06	869.35	10.48	9.68
Transparent	0.62	1454.02	53.06	52.93

wide occurrence of  $\text{Ti}^{3+}$  as minor impurity in minerals has been commonly detected by EPR (Marfunin, 1979). Like the other  $d^1$  ions ( $\text{V}^{4+}$ ,  $\text{Mo}^{5+}$ ),  $\text{Ti}^{3+}$  ions occur often in minerals in the form of electron centers. It may occur in benitoite, which has been exposed to gamma rays in its natural setting. There could be radiation centers, such as, for example,  $\text{Ti}^{4+} + \text{gamma ray} + \text{electron donor} \Rightarrow \text{Ti}^{3+} + \text{electron hole}$ . The color of benitoite does not change with gamma irradiation to quite high doses (Rossmann, 1997), but luminescence can occur from centers at such low concentration though they do not influence the color of benitoite.

Figure 5a shows the energy level scheme of octahedrally coordinated  $\text{Ti}^{3+}$  ions in the presence of cubic, tetragonal or orthorhombic crystal field distortions (Yamaga et al., 1992). The  ${}^2D$  state of  $3d^1$  ions in an octahedral field splits into the  ${}^2T_2$  ground state and the  ${}^2E$  excited state with energy separation  $10D_q$ . In tetragonal symmetry, the  ${}^2T_2$  ground state is further split into the  ${}^2B_2$  and  ${}^2E$  states. Which of the orbital doublet ( ${}^2E$ ) or the singlet ( ${}^2B_2$ ) is lower is determined by whether the octahedron is elongated or compressed, respectively, along the z-axis. The  ${}^2E$  excited state is split further into  $A_1$  and  $B_1$  states by tetragonal distortion. If the octahedral complex of the  $\text{Ti}^{3+}$  ion is compressed, the  $B_1$  state is lower in energy. The  ${}^2T_2$  state in orthorhombic symmetry splits into three non-degenerated

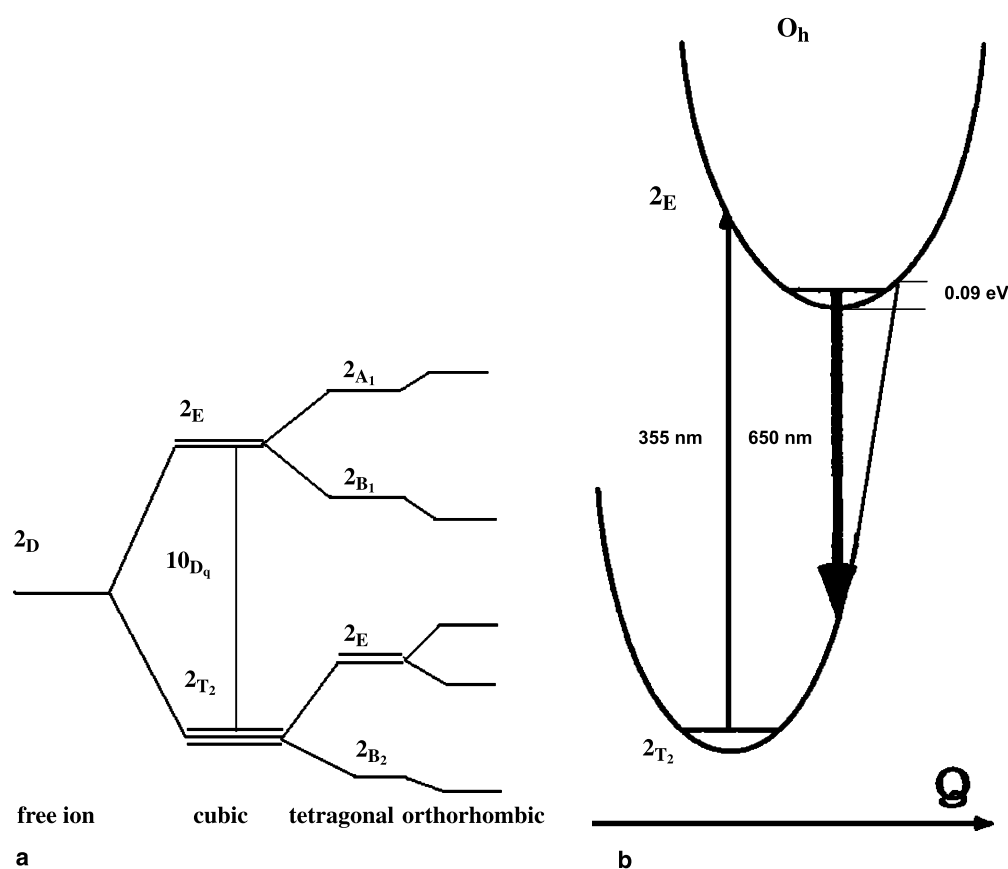


Fig. 5. **a** Energy level scheme of  $\text{Ti}^{3+}$  in cubic, tetragonal and orthorhombic symmetries (Yamaga et al., 1992); **b** Configurational coordination diagram for  $\text{Ti}^{3+}$  in benitoite

orbital states. The lowest excited state in orthorhombic symmetry is represented by a linear combination of the  $A_1$  and  $B_1$  states. The mixing coefficients are determined by the strength of the crystal field perpendicular to the dominant tetragonal field. For example, in sapphire crystals, the  $Ti^{3+}$  luminescence at room temperature is characterized by a strongly polarized band peaking at approximately 750 nm with a decay time of 3.1  $\mu s$  (Fabeni et al., 1991).  $Ti^{3+}$  substitutes for the  $Al^{3+}$  ion of the host crystal in a trigonally distorted lattice site; the strong crystal field has cubic- and trigonal-symmetry components. The splitting of the  ${}^2E$  state is the reason for a double-peaked visible absorption band, whereas no splitting is observed in the emission band.

Intensity and decay time temperature dependence of the benitoite luminescence band at 650 nm may be interpreted using the energy level scheme of the  $Ti^{3+}$  luminescence center. The excitation peak at 350 nm is connected with the  ${}^2T_2-{}^2E$  transition, while the splitting of the  ${}^2E$  state is the reason of the two shoulders in the excitation spectrum. At lower temperature the opposite transition generates the intense luminescence band peaking at 650 nm with a decay time of 20  $\mu s$ . Thermal quenching and drastically reduced decay time with increasing temperature result from non-radiative transitions from the excited to ground state (Fig. 5b). Similar behavior is known in titanium doped YAG, where the  $Ti^{3+}$  ion has different site symmetry from that in sapphire, as Ti is incorporated in YAG at the trigonally-distorted octahedral Al site with inversion symmetry (Fabeni et al., 1991). In this case, for the luminescence band peaking at 760 nm the radiative lifetime of 50  $\mu s$  at 4.2 K is drastically reduced to 2  $\mu s$  with increasing temperature.

The main difference between the red benitoite luminescence at 650 nm and the  $Ti^{3+}$  emission in  $Al_2O_3$  and  $Y_3Al_5O_{12}$  is the strong blue shift of the benitoite emission, and especially of the excitation bands. For example, the excitation and absorption maximum of  $Ti^{3+}$  in sapphire is at 550 nm, while in benitoite it is at 355 nm. Nevertheless, such variation is not so uncommon for  $Ti^{3+}$  to be present in different matrixes. For example, a strong absorption in the region 260–280 nm was observed in the  $Al_2O_3-Ti^{3+}$  crystals attributed to a high  $Ti^{3+}$  concentration (Wong et al., 1995). Besides, the optical absorption spectrum of  $Ti^{3+}$  in  $YAlO_3$ , where  $Ti^{3+}$  substitutes for  $Al^{3+}$  in sites with orthorhombic symmetry, is composed of two broad bands with peak wavelengths of 434 and 492 nm, the energy separation of which is due to splitting of the excited  ${}^2E$  state, while the broad-band luminescence has a maximum at 605 nm (Yamagi et al., 1992). Such absorption and luminescence parameters are closer to those found in benitoite. Nevertheless, the UV excitation band, the large blue shift of the emission band and very high Stokes shift demand additional argumentation on  $Ti^{3+}$  participation in the red benitoite luminescence. A promising way may be the luminescence correlation with EPR method capable of unequivocal  $Ti^{3+}$  identification.

#### *Band at 730 nm and narrow line at 682 nm – $d^3$ elements related luminescence*

Time resolved spectroscopy at 300 K under different excitations with different decays and gates revealed that both the band at 730 nm and the line at 682 nm behave

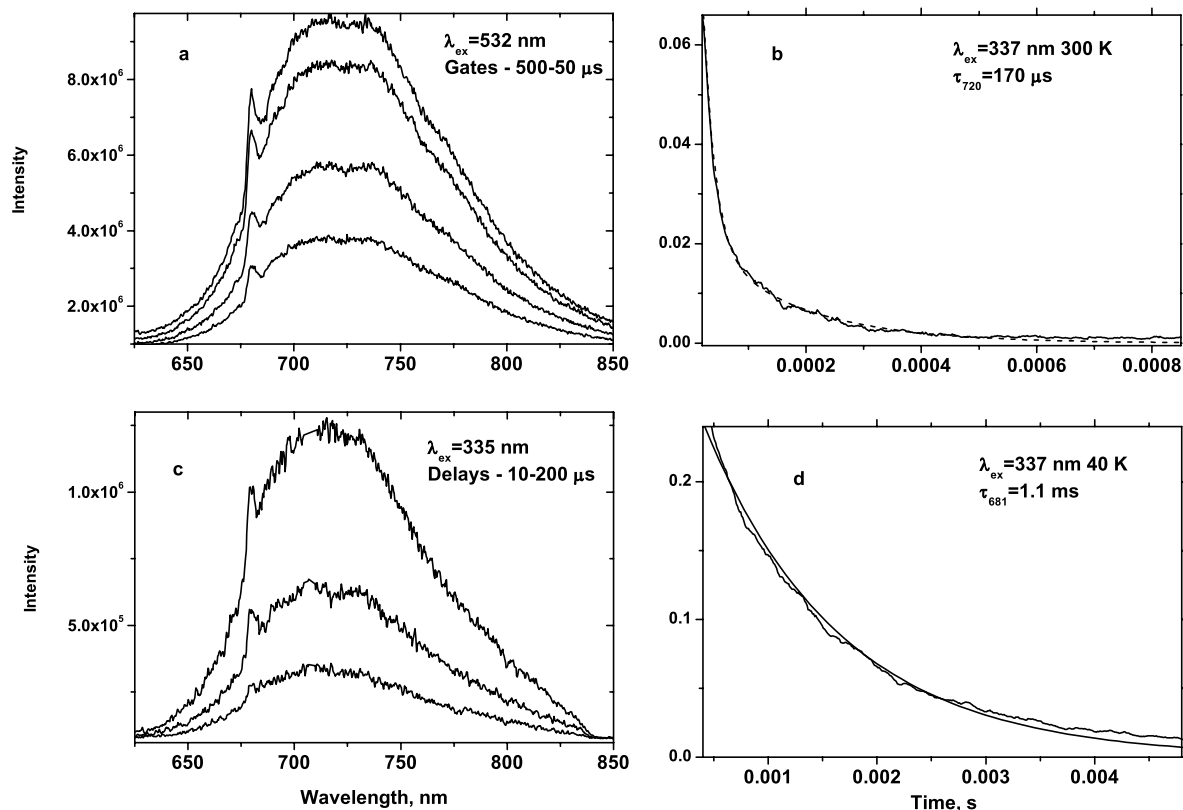


Fig. 6. Long wavelength red luminescence of transparent benitoite: **a** emission spectrum at room temperature under 532 nm excitation with different gates, changing from 500 to 50  $\mu\text{s}$ ; **b** decay time of the band at 730 nm under 337 nm excitation at 300 K; **c** emission spectrum at room temperature under 335 nm excitation with different delays, changing from 10 to 200  $\mu\text{s}$ ; **d** decay time of the line at 682 nm under 337 nm at 40 K

in a similar way, namely they have similar decay time of  $\sim 170 \mu\text{s}$  (Fig. 6a–c). The broad band is quenched at low temperatures, while the narrow line is much stronger at lower temperatures, where two additional weak lines appear at 695 and 702 nm, respectively (Fig. 2a). The decay time at low temperature is very long, reaching 1.1 ms at 40 K (Fig. 6d).

Combination of broad emission band and narrow line is typical for elements with  $d^3$  electronic configuration. The most important free ion states for  $d^3$  ions are  $^4F$  ground level and excited  $^2H$  level. In an octahedral field, the  $^4F$  level splits into the  $^4A_2$  ground state and the excited  $^4T_2$  and  $^4T_1$  states. The spin allowed transitions that could therefore be used to populate the excited states directly correspond to  $^4A_2 \rightarrow ^4T_2$  and  $^4A_2 \rightarrow ^4T_1$ .

The best-known luminescence center of  $d^3$  type in minerals is  $\text{Cr}^{3+}$ , which mainly appears in minerals as a trace constituent substituting for  $\text{Al}^{3+}$  in six-fold coordination (Tarashchan, 1978). As such, the larger  $\text{Cr}^{3+}$  ion is placed in a site with small metal–ligand distances and the crystal field is large, typically 1650–1750  $\text{cm}^{-1}$ . If the crystal field is sufficiently strong to make the doublet state the excited state with lowest energy, there will be a red luminescence. Because the

doublet state belongs to the same orbital configuration as the ground state, the Stokes shift and Condon offset will be small. As a result, the line width of emission is narrow and a considerable amount of phonon fine structure is observed even at room temperature. Such transition is forbidden by symmetry and spin selection rules, and decay time is usually very long. Although the narrow emission line is essentially independent of crystal field and thus of site size and symmetry, the energy of the double levels does depend on Racah parameters B and C, which are dependent on the covalence of the metal–ligand bond and thus there is some variability in the line emission from mineral to mineral. At weaker crystal fields, a strong broadband quartet–quartet  ${}^4T_2 \rightarrow {}^4A_2$  transition appears. It is characterized by a broad red emission band and only symmetry forbidden, thus has a much shorter decay time.

For the intermediate crystal field sites, for which the crystal field parameters lie in the crossing region of the  ${}^4T_2$  and  ${}^2E$  states, there is mixing between doublet and quartet states resulting in complicated spectra, non-radiative transfer and considerable temperature dependence. In such case the emission from both  ${}^4T_2$  and  ${}^2E$  states may be expected. It is possible that spin-orbit interaction, coupling  ${}^2E$  and  ${}^4T_2$  states, could be responsible for breaking of the selection rule forbidding the  ${}^2E \rightarrow {}^4A_2$  transition. The admixture of the  ${}^4T_2$  wave function into the  ${}^2E$  wave function, which depends on the doublet–quartet energy separation, determines the radiative lifetime of the doublet, which may therefore change significantly with crystal field. Thus the broad band connected with the  ${}^4T_2$  transition, and the narrow line connected with the  ${}^2E$  transition, have very similar decay time, which is what is obtained in benitoite. At 300 K the lower  ${}^2E$  state acts as an energy reservoir for the  ${}^4T_2$  state and thermal activation enables emission mainly from the  ${}^4T_2$  level. At lower temperatures the thermal activation is impossible and the  ${}^2E$  level becomes luminescent.

Nevertheless, not only  $Cr^{3+}$  is capable to generate such kind of luminescence. Similar behavior is typical of other  $d^3$  elements such as  $Mn^{4+}$ . Possible participation of manganese is supported by its presence in benitoite samples studied (Table 1). Such concentrations are quite sufficient for luminescence generation. Substitution in the form of  $Mn^{2+}$  for  $Ba^{2+}$  is doubtful because of the great difference in ionic radii. In artificial phosphors luminescence bands due to  $Mn^{4+}$  exist from 620 to 715 nm. The spectrum has a structure consisting of several broad lines originating from transitions aided by lattice vibrations. Because the crystal field at the higher charged  $Mn^{4+}$  ion is stronger than that for  $Cr^{3+}$ , the emission is most probably connected with the  ${}^2E \rightarrow {}^4A_2$  transition, but in many cases the origin of the emitting and ground states is doubtful (*Blasse and Grabmaier, 1994*).

## Conclusions

The red luminescence of benitoite is much less known compared to its blue emission. Nevertheless, it appears to be the first case where the participation of  $Ti^{3+}$  emission in mineral luminescence must be seriously considered. This conclusion is possible as a result of time-resolved luminescence spectroscopy analysis of the changes of emission band form, intensity and decay time with changing temperature. An additional center of red emission in benitoite is connected with a  $d^3$  transition element, most probably  $Cr^{3+}$  or  $Mn^{4+}$ .

## References

- Blasse G, Grabmaier B* (1995) Luminescent materials. Springer, Berlin Heidelberg New York, 233 pp
- Fabeni P, Pazzi G, Salvini L* (1991) Impurity centers for tunable lasers in the ultraviolet and visible regions. *J Phys Chem Sol* 52: 299–317
- Gaft M, Reisfeld R, Panczer G, Boulon G* (2001) The luminescence of Bi, Ag and Cu in natural and synthetic barite BaSO<sub>4</sub>. *Opt Mat* 16: 279–290
- Gaft M, Nagli L, Reisfeld R, Panczer G* (2003) Laser-induced time-resolved luminescence of titanite. *Opt Mat* 24: 231–241
- Gaft M, Nagli L, Waychunas G, Veiss D* (2004) The nature of blue luminescence of natural benitoite BaTiSi<sub>3</sub>O<sub>9</sub>. *Phys Chem Minerals* 31: 365–373
- Khomenko V, Langer K, Rager H, Fett A* (1998) Electronic absorption by Ti<sup>3+</sup> ions and electron delocalization in synthetic blue rutile. *Phys Chem Minerals* 25: 338–346
- Laird J, Albee A* (1972) Chemical composition and physical, optical, and structural properties of benitoite, neptunite, and joaquinite. *Am Mineral* 57: 85–102
- Laurs BM, Rohtert WR, Gray M* (1997) Benitoite from the New Indria District, San Benito County, California. *Gems & Gemol* 33: 166–187
- Louderback G* (1909) Benitoite, its paragenesis and mode of occurrence. University of California Publication. *Bull Dept Geol* 5: 331–380
- Marfunin A* (1979) Physics of minerals and inorganic materials. Springer, Berlin Heidelberg New York
- Rossmann G* (1997) <http://minerals.gps.caltech.edu/>
- Tarashchan A* (1978) Luminescence of minerals. *Naukova Dunka* (in Russian)
- Vassilikou-Dova A, Eftaxias K* (1991) Paramagnetic defects in benitoite. *Z Naturforsch* 46: 579–582
- Wong W, McClure D, Basun S, Kokta M* (1995) Charge-exchange processes in titanium-doped sapphire crystals. *Phys Rev B* 51: 5682–5693
- Yamaga M, Yosida T, Henderson B, O'Donnell K, Date M* (1992) Electron paramagnetic resonance and optical spectra of Ti<sup>3+</sup>-doped YAlO<sub>3</sub>. *J Phys Cond Mat* 4: 7285–7294

Authors' addresses: *M. Gaft* (corresponding author; e-mail: michael\_g@itlasers.com), The Open University of Israel, 108 Ravutski St., Raanana, Israel; *L. Nagli*, School of Physics and Astronomy, Tel-Aviv University, Tel-Aviv, Israel; *G. Waychunas*, Geochemistry Department, Aqueous Geochemistry Group, Earth Sciences Division MS 70-108B E.O. Lawrence Berkeley National Laboratory, One Cyclotron Road, Berkeley, CA 94720, USA; *G. Panczer*, Physical Chemistry of Luminescence Materials Laboratory, Lyon 1 University, UMR 5620 CNRS, 43 Bd du 11 November 1918, 69622 Villeurbanne, France